

Developing A Method for Inter-Seed Effect Correction in ^{125}I Interstitial Brachytherapy Using Artificial Neural Network

Kheibar Bayati¹, Sedigheh Sina^{1,2,*}, Reza Faghihi¹, Vahed Moharramzadeh¹, Maryam Papie¹

1. Nuclear Engineering Department, School of Mechanical Engineering, Shiraz University, Shiraz, Iran.
2. Radiation Research Center, Shiraz University, Shiraz, Iran.

ARTICLE INFO

Article type:
Original Paper

Article history:
Received: Jul 01, 2020
Accepted: Jan 05, 2021

Keywords:
Dosimetry
Monte Carlo Method
Interstitial Brachytherapy

ABSTRACT

Introduction: Treatment planning systems use TG-43 dose calculation protocol for brachytherapy sources. Dose calculations based on TG-43 formalism do not correct the perturbations due to the presence of tissue inhomogeneity, applicators, and inter-seed effects. Inter-seed attenuation has an important effect on dosimetry in permanent implant brachytherapy. The aim of this study is to evaluate the inter-seed attenuation effect for I-125 permanent implants. Then, software was developed to find the real dose distribution for different combinations of sources.

Material and Methods: In the first step, a hypothetical generic source model was designed based on the configurations of different commercial source types. MCNP5 Monte Carlo code was utilized to simulate the single active generic source at the center of the phantom, and an inactive placed at various positions inside the phantom. An algorithm was introduced using artificial neural network models that can estimate the dose distribution in presence of inactive sources.

Results: The Monte Carlo calculation results showed that the dose distribution is affected by the inter-seed attenuation effect. Comparison of the artificial neural network results with the Monte Carlo simulation results show that the artificial neural networks can predict the inter-seed attenuation with acceptable accuracy. Comparison of the MC calculations, and the ANN output does not show statistically significant differences between the results (P value>0.95).

Conclusion: Inter-seed effect is dependent on the distance between the seeds. Decreasing distances would cause more effect. According to the results, it seems that the artificial neural network can be used as a tool for correction of inter-seed attenuation effect in treatment planning systems.

► Please cite this article as:

Bayati Kh, Sina S, Faghihi R, Moharramzadeh V, Papie M. Developing A Method for Inter-Seed Effect Correction in ^{125}I Interstitial Brachytherapy Using Artificial Neural Network. Iran J Med Phys 2022; 19: 14-21. 10.22038/IJMP.2021.50066.1814.

Introduction

Brachytherapy is one of the main effective radiation modalities used to treat various cancerous tissues such as the brain, head and neck, uterus, cervix, etc [1]. Irradiations from sealed radioactive sources can be applied with interstitial, intracavitary or surface mold modalities to deliver the prescribed dose near the sources in a tumor. Rapidly decreased dose after tumor, provides a local high dose region at the malignancies with normal tissue protection [2]. Based on the required dose values, various types of brachytherapy methods including permanent or temporal source implants are available to choose with suitable dose rates for the transmission of the irradiations [3]. The treatment planning scope is providing an optimal dose distribution for the tumor and sufficient protection at normal tissues. Achievement of this purpose requires an accurate dose calculation formalism that considers the real treatment conditions. However, most commercial treatment planning systems perform the dosimetry calculations based on the recommendation of the American Association of Physics in Medicine Task

Group No. 43 (AAPM TG-43). AAPM TG-43 uses a simple water phantom without any corrections for scattering and absorption effects of the incident photons on applicators, sources and tissue inhomogeneities. AAPM TG-43 recommends a superposition method based on the summation of all single source dose distribution, each calculated separately. Hence, dosimetry for different combinations of several sources (multi-seed implants) in brachytherapy can be significantly affected by the attenuations due to the presence of other seeds. Ignorance of the inter-seed attenuations and source self-absorption effects that make a lowered accuracy in dose calculations has more serious effects in permanent implants with low energy applications. Low energy sources because of needing less shielding; and those with a short half-life for their biologic advantages make them a suitable selection to use as permanent implants in brachytherapy. I-125 with a half-life of 59.4 days and weighting mean photon energy 28.37 Kev, is a common source in permanent interstitial implants [2, 4, 5]. There are several studies,

on evaluation of the attenuations due to the sources and especially their shields. Sina et al. in a Monte Carlo (MC) simulation for low dose rate (LDR) Cs-137 (model Selectron), investigated a correction factor to introduce the applicator shielding effects on TG-43 dosimetric parameters [6]. Additionally, a correction factor for dosimetric differences in various tissues related to the water was produced [7]. Meigooni et al. have performed a dosimetry investigation on interstitial brachytherapy sources based on AAPM TG-43 recommendations. They considered two linear configuration multi-seed plans with three seeds in longitudinal and transverse planes. I-125 6702 and I-125 6711 model sources were selected for each one. Their results demonstrated a mean reduction of 6% for the sum of doses from individual sources. Estimations that were found with different values in longitudinal and transverse planes were validated with TLD measurements [8]. In another study, Mason et al. considered the effects due to inhomogeneous tissues and inter-seed attenuation and scatter for I-125 seeds in prostate implant brachytherapy. The required corrections were evaluated based on dose-volume histogram (DVH) analysis. Uncertainties were less than 0.5% for patients without calcification and up to 4% for those with calcification [9]. An algorithm to determine the inter-seed attenuation in LDR brachytherapy is presented by Safigholi et al. [10].

In recent years, artificial neural networks, and deep learning have been proposed by different investigators in different fields of medical physics [11,15]. It has been shown that the deep learning can be used in brachytherapy dosimetry, and treatment planning. Accurate dosimetry can be performed close to those of the MC algorithm, but with much faster computation times [13-15].

The purpose of this study is to evaluate the application of artificial neural networks in evaluating, and correcting of the inter-seed attenuation effect in treatment planning systems. The investigation was performed for permanent brachytherapy implants by presenting a hypothetical generic source model using MC simulation and an artificial neural network.

Materials and Methods

This study was performed in three main steps including 1) the geometry and materials in different I-125 source types were compared to introduce a generic seed model. This generic model is a hypothetical I-125 source that is representative of other sources. By defining this generic model, we don't have to repeat the simulations for all I-125 seed models. 2) The generic model was used to investigate the inter-seed attenuation effect. 3) The dose estimation software was created using artificial neural networks. The steps are spaciouly described in the following sections.

Defining a generic source model

The geometry and composition of different commercially available I-125 sources (see Table 1) were used to define a generic source Model. The designed generic model was then used as a hypothetical ^{125}I source in Monte Carlo simulations; thus, we didn't have to simulate each individual sourced model. Mean dimensions and most frequently used materials were utilized for introducing two generic models. The dose distribution around the generic sources was compared with commercially available sources to choose one generic model as I-125 seed.

MCNP5 simulation for evaluation of the inter-seed effect

Monte Carlo N-Particle MCNP5 code was used for the investigation of the dose distribution around the I-125 generic seed. To evaluate the dose distributions, as shown in figure 1, a cubical soft tissue phantom ($\rho=1.04 \text{ g/cm}^3$) with the dimension of $8 \times 8 \times 8 \text{ cm}^3$ was simulated inside a sphere of air ($\rho=1.00121 \text{ g/cm}^3$ and radius of 7 cm). The active source was placed at the center of the phantom.

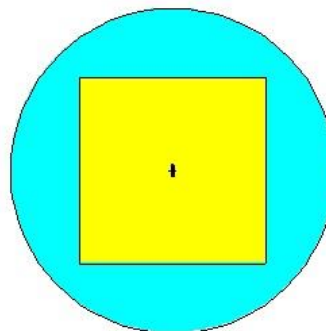


Figure 1. The simulated phantom

The dosimetry parameters of the generic seed model were obtained based on the updated TG-43 report (TG-43U1) [6]. MCNP5 simulation was performed with 10^9 particles to assess the absorbed dose inside the cubical phantom in mesh tally cells. The MCNP simulation results showed the relative error of less than 1% for each tally cell. The dose at different points was obtained by the production of *FMESH4 tally and appropriate mass absorption coefficient. Dose distribution plots were provided using MATLAB software from a data matrix involving $99 \times 99 \times 99$ small cubes (0.8 mm resolution). Then an inactive generic source was assumed at the various distances and angles from the active generic source. Active source located at the center of the phantom ($x=0, y=0, z=0$). 15 dwell positions for inactive sources were considered to evaluate the inter-seed attenuation effect for different usual distances within the treatment volume in permanent implant brachytherapy. Inactive sources were simulated as parallel with the active source axis. Figure 2 shows an examined manner with the inactive source at point (0.58 cm, 0cm, 0cm).

Table 1. The characteristics of different commercial I-125 seed models

I-125 source type	Marker substance*	Marker dimension (mm)	Shape of source absorbent marker	Capsule end thickness (mm)	Capsule wall thickness (mm)	Capsule substance	Active length (mm)	Capsule width (mm)	Capsule length (mm)
6702	Resin	d=0.6	3 spheres	0.4	0.05	Titanium	3.30	0.8	4.5
6711	Silver	L=3 d=0.5	1 cylinder	0.4	0.05	Titanium	2.80	0.8	4.5
IS-12501	Resin	d=0.6	5 spheres	0.4	0.05	Titanium	3.40	0.8	4.5
SL-125SL-125	Resin	d=0.5	5 spheres	0.3	0.05	Titanium	3	0.8	4.5
MED 3631	Resin	d=0.5	4 spheres	0.15	0.05	Titanium	4.2	0.8	4.5
Best 2301	Tungsten	L=3.95 d=0.25	1 cylinder	0.05	0.1	Titanium	3.95	0.8	5
125.S06	Gold marker + Ceramic coating	L=3.5 (Ceramic D=0.6) (gold marker: d=0.17)	1 cylinder	0.4	0.05	Titanium	3.5	0.8	4.5
DraxImage LS-1	Resin	d=0.5	2 spheres	0.05	0.1	Titanium	4.1	0.8	4.5
STM125 1	Gold core + Aluminum layer	L=3.81 (Alumin wire D=0.5) d=0.36	1 cylinder	0.13	0.08	Titanium	3.8	0.8	4.5
3500	Silver core + Quartz tube	L=3.76 (Quartz tube: D=0.64) (Silver marker: d=0.406)	cylinder	0.25	0.05	Titanium	3.76	0.8	4.5

* L is the length of marker (for cylindrical markers), d is the diameter of markers (for cylindrical, and spherical markers), and D is the external diameter of the layer, covering the marker for some cylindrical markers.

Artificial neural network for prediction of the inter-seed effect

A neural network model tries to produce an electronically computational method based on the biological behavior patterns of the human brain neural system [16]. In the last step, a method was developed for correcting the inter-seed effect using an artificial neural network. For this purpose, the Artificial Neural Network Toolbox of MATLAB 2014a software was used. Levenburg-Marquardt backpropagation algorithm was employed, and mean-Square Error was used for obtaining the accuracy of the model, and the reliability was tested using regression.

As stated in the previous section, the dose distribution in presence of inactive seeds located at different positions was obtained using MCNP5 Monte Carlo simulation. The position of the inactive seeds relative to the active one, and the dose distribution around the source was inserted to train the network.

The input data matrix was restricted to the first quarter of the plane including a 2D 50×50 portion. To shorten the computational process, the input matrix was reduced by the elimination of secondary rows and columns (a 25×25 matrix for each source position, 15×625=9375 data cell in each input matrix). Network results will be true for the same target and inputs in the other quarters.

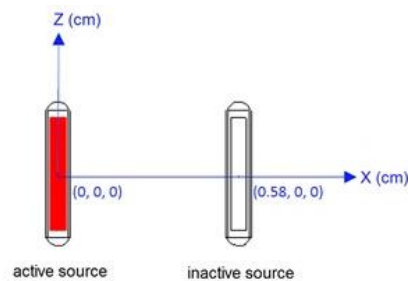


Figure 2. Dwell positions for the active source (red color for the active region) and inactive source

Results

Generic seed definition

Proposed generic models are introduced as in Table 2. The properties were defined based on the dimension, geometry and shape of the commercially available seeds shown in Table 1. These two generic source models are only different in their marker substances. To choose the appropriate marker substance between Resin and Tungsten, a dosimetry study was performed by MCNP5 simulation. The dose distribution around the generic sources was compared with the dose around each source model.

Table 2. Two generic seed models defined in this study

	Marker substance*	Marker dimension (mm)	Shape of source absorbent marker	Capsule end thickness (mm)	Capsule wall thickness (mm)	Capsule substance	Active length (mm)	Capsule width (mm)	Capsule length (mm)
Generic seed #1	Resin	L=3.6 & d=0.5	cylinder	0.25	0.06	Titanium	3.6	0.8	4.6
Generic seed #2	Tungsten	L=3.6 & d=0.5	cylinder	0.25	0.06	Titanium	3.6	0.8	4.6

* L is the length of marker, d is the diameter of markers.

According to the results, the minimum deviation in dosimetry parameters of the real commercial seeds and the generic sources was observed in the case of resin marker. Therefore, generic seed #1 was used for the following steps of this study, as the representative generic seed model. The dose distribution around this generic source model is shown in figure 3.

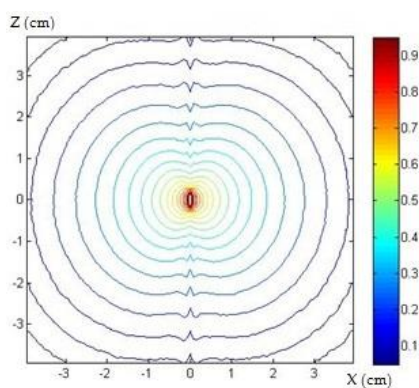


Figure 3. The dose distribution around the generic source model

MCNP5 simulation for evaluation of the inter-seed effect

At the next step of the evaluations, the dose distribution around the active source affected by the inactive one was investigated. Dose distribution were considered for inactive source positioned at the points of (x(cm), y(cm), z(cm)): (0.58, 0, 0), (1.58, 0, 0), (3.58, 0, 0), (0, 0, 1), (0.58, 0, 1), (1.58, 0, 1), (3.58, 0, 1), (0.58, 0, 2), (1.58, 0, 2), (3.58, 0, 2), (0.58, 0, 3), (1.58, 0, 3), (3.58, 0, 3), while the active one is at point (0,0,0). Figure 4 shows the obtained results about the effects of inactive pellets located at different distances on the dose distribution around the active seed.

As seen in figure 4, the shielding effect of the secondary source has clearly had the attenuating effect. This effect is observed as dependent on the distance between both sources. The inter-seed effect increases by decreasing the distance between the active seed and the inactive one. Therefore, it seems that precise dosimetry will not be performed by ignoring the inter-seed attenuation effect.

Prediction of the dose distribution using ANN

The artificial neural networks were used for obtaining the dose distribution around the seeds in the presence of different inactive source positions.

First, a network was created for the input matrix of inactive source positions and the output matrix of dose values.

A regression plot was used to check how well the input and output network data are fitted. In this study, 60 percent of the provided data were used for training, and 40 percent of the data were used for testing the network. Regression plot for the train, and test datasets of this network is shown in Figures 5a, and 5b. Figure 5c shows the regression plot for all the data. From these graphs, one can observe that the data sets used for training and testing the network are properly fitted to the lines, which approves the accuracy of the network results. Such plots can be used for predicting the output for every other input data. As shown in the figure, an accurate method with good agreement between the value obtained with the trained artificial neural network and the true values are obtained. Additionally, the network performance curve shows an acceptable difference with the best training performance (Figure 6).

Validation of the artificial neural network model was performed by comparing the dose distributions around the source obtained by the model with the Monte Carlo simulations. Comparison was first performed for 13 inactive source positions that were considered to generate the network. Figure 7a, exhibits the isodose curves for the plan with the inactive source placed at (1.58cm, 0cm, 0cm). Based on the results, for all given positions, the model is highly consistent with the MC calculations with provided percentage differences of less than 1%.

The artificial neural network must be validated for every possible position of the inactive source. Thus, comparisons were repeated for the other positions than those used in network production. For our example inputs, MC simulation was performed for the inactive source positions (1.75cm, 0cm, 2.5cm) and (0cm, 0cm, 1.5cm), then the network was examined to find the dose distributions. Figure 8 shows the obtained isodose curves. The consequence percentage differences are also plotted in figure 9.

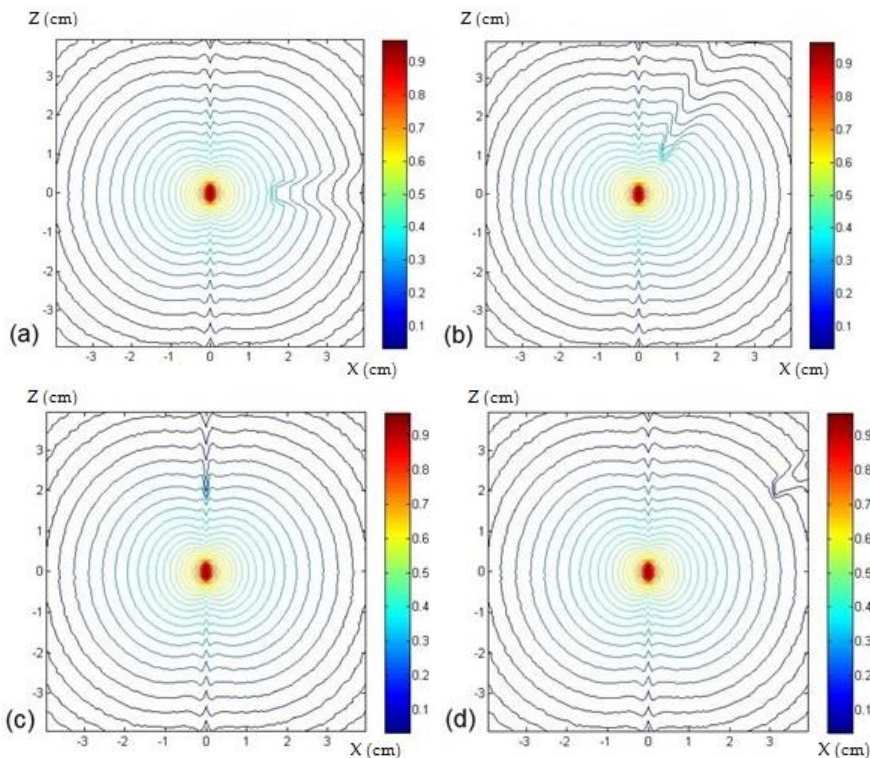


Figure 4. The dose distribution around the centered active source with the presence of inactive source at the points a: (1.58cm, 0cm, 0cm), b: (0.58cm, 0cm, 1cm), c: (0cm, 0cm, 2cm) and d: (3.08cm, 0cm, 2cm)

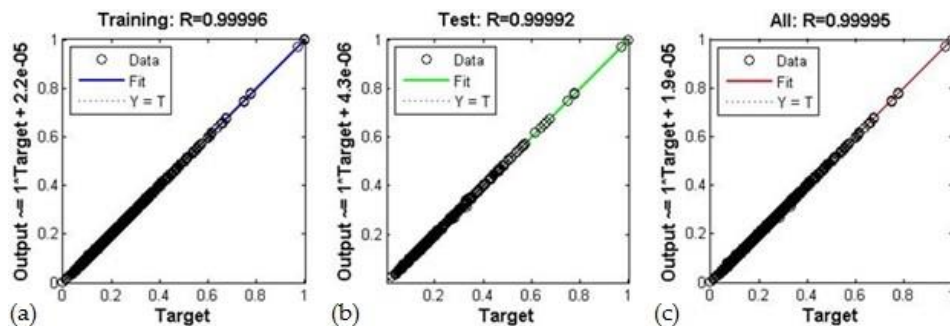


Figure 5. Regression between the first network results and MC calculations, a) for the training b) for testing, and c) for validation data

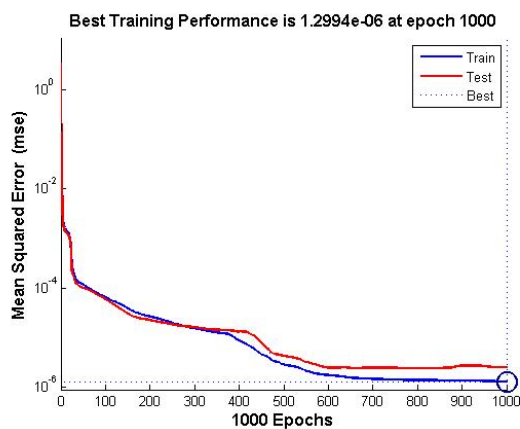


Figure 6. Performance curve of the created network, the mean square error for the training, and testing set for different epochs

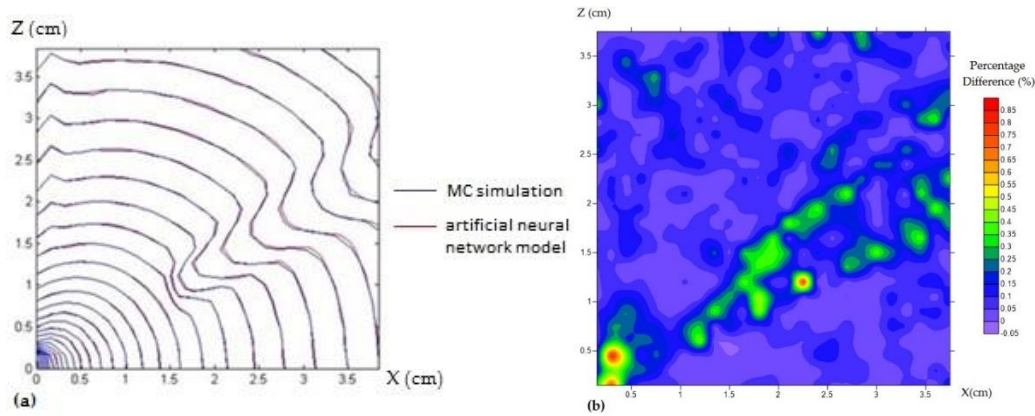


Figure 7. a) Dose distribution in X-Z coordinate (1.58cm, 0cm, 0cm); b) percentage Difference between Monte Carlo simulation and artificial neural network model; for the plan with inactive source position

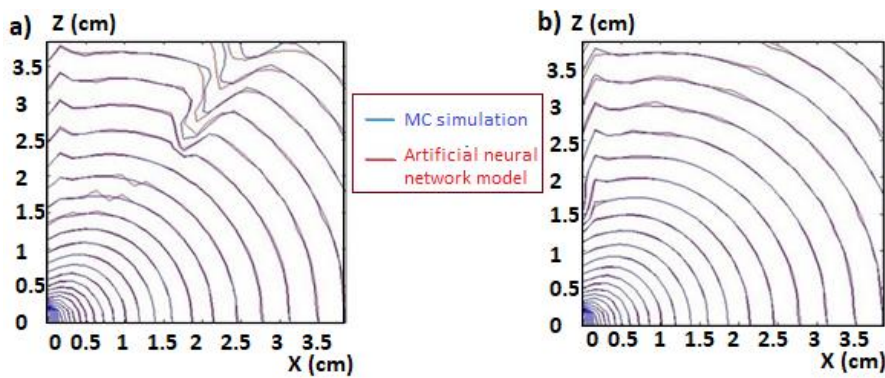


Figure 8. The dose distributions, in X-Z coordinate, produced by MC simulation and artificial neural network model for two cases with inactive source positions at a: (1.75cm, 0cm, 2.5cm) and b: (0cm, 0cm, 1.5cm)

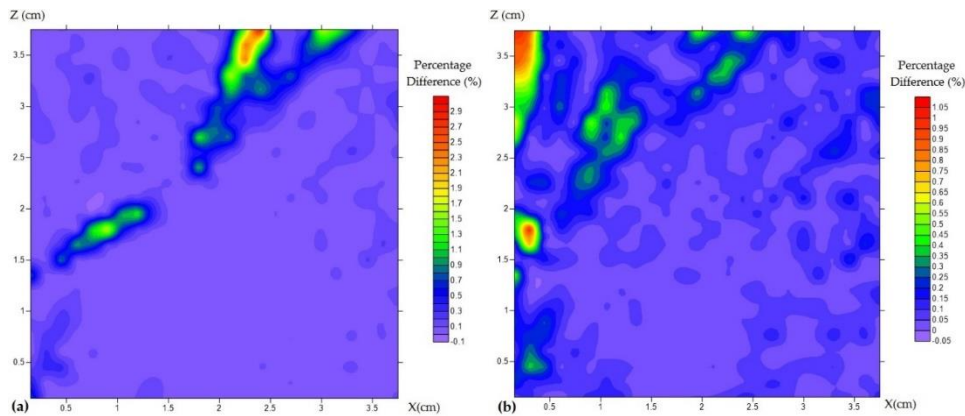


Figure 9. Percentage difference for artificial neural network model related to MC simulation for the plan with inactive source positions at a: (1.75cm, 0cm, 2.5cm) and b: (0cm, 0cm, 1.5cm)

According to the results shown in Figure 9 observed for both inactive seed positions, the percentage differences were not much greater than about 3% in all dosimetry points. The statistical analysis of the values obtained by the MC results, and the ANN are similar, P value>0.95. This shows accurate estimations around the active source in multi-seed implants for every other point of tissue that was not used in the artificial neural network generation process.

In real treatment situations, there are several active sources, causing the inter-seed attenuation. Therefore, the

ability of the neural network for prediction of dose distribution around a source with several other dummy seeds around itself was examined too. The active source is located at (0cm, 0cm, 0cm), and three dummy pellets were positioned at (1.58cm, 0cm, 3cm), (3.08cm, 0cm, 2cm), and (3.08cm, 0cm, 0cm). Figure 10 compares the predicted dose distribution, with the MC simulations that the results have shown again that the neural network was able to predict the inter-seed effect with less than 2% deviation.

Therefore, the validated method was developed for the prediction of dose distribution in real brachytherapy treatments contained using several active seeds. This model produces the dose distribution around each active source by TG-43U1 formalism. Then the dose distribution is corrected for the inter-seed effect using the trained network. Finally, the corrected dosimetry is performed by the superposition of the dose around each source. Figure 11 shows the neural network training window.

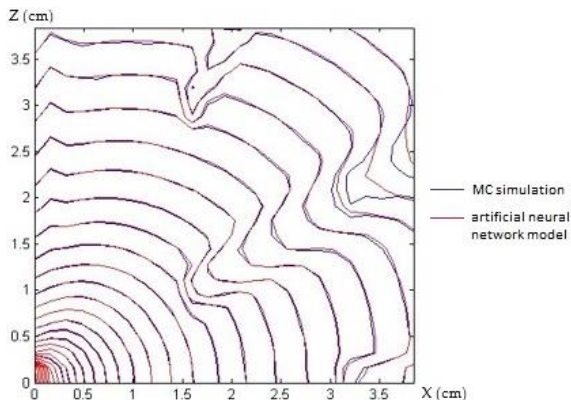


Figure 10. The dose distribution in X-Z coordinate, produced by MC simulation and artificial neural network model for the plan with inactive source positions at (1.58cm, 0cm, 3cm), (3.08cm, 0cm, 2cm), and (3.08cm, 0cm, 0cm)

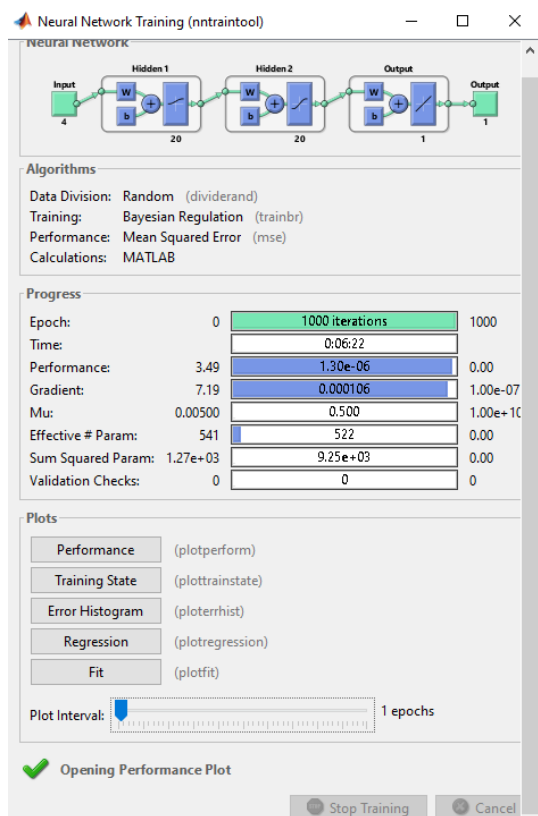


Figure 11. Neural network training window

Discussion

In low energy photon emitting brachytherapy sources, ignoring inter-seed effect would cause significant errors in dose calculations, especially when high atomic number materials are used in the brachytherapy seed structure. This is because the photoelectric effect is dominant in low energy photon range for which the cross-section varies as Z^4 , where Z is the effective atomic number of the material. In this study, artificial neural networks were applied for the evaluation and prediction of the dose distribution around low energy brachytherapy sources. MCNP5 Monte Carlo simulations were employed to produce a dosimetry dataset as the required initial data for machine learning. The ability of artificial neural networks in predicting the inter-seed effect was then evaluated. According to the results of this study, the ANN is capable of finding dose plots for inputs including cartesian coordinates (x, y, z) of the active seed dwell positions. The results of this investigation indicate that dose distribution around active sources will be affected by the presence of the other sources. The effects are highly dependent on the secondary source position relative to the considered active source. The greater inter-seed attenuation effect is found for the seeds located near each other. These corrections that were evaluated in two-dimensional plots, can be also done in three-dimensional dose distributions as well as optimized source localizations.

Some high-Z materials are used in the construction of brachytherapy seeds, therefore the dose distribution around the low-energy seeds is affected significantly in presence of other brachytherapy seeds. The dosimetry calculations based on AAPM TG-43 formalism which uses the superposition principle, and ignore the inter-seed attenuation effects, can produce significant uncertainty in dose distribution around the sources. Most treatment planning systems use the TG-43 formalism, and the inter-seed effect is ignored. Meigooni et al 1992, found that the average value of the inter-seed effect was 6% for I-125 seeds, with a maximum of 12%. Mason et al, 2014 showed that the inter seed and tissue effect could change the D_{90} of the prostate by 2.9%, and D_{2cc} of the rectum by 10.5% [9]. The results of this study showed the interseed effect of 2 to 10%, which is in agreement with the previous investigations. The artificial neural networks used in this study can be used for the correction of the dosimetry errors. The Monte Carlo simulation results were used as the dataset for training the network. The artificial neural network that uses the source positions as network inputs, shows a good accuracy in predicting the real dose distribution around the source in multi-seed implants. This algorithm can provide dose distributions with less than 5% deviations related to the MC simulations.

Conclusion

This study shows the benefits to use artificial neural networks for dosimetry purposes. It seems that artificial neural networks can be successfully used for accurate

dosimetry with inter-seed attenuation effect correction for AAPM TG-43-based dose calculation. Currently, artificial intelligence is being widely used in external radiation therapy, and brachytherapy dosimetry, and treatment planning. For more studies, efforts can be focused on developing dosimetry calculation using artificial neural networks, applied as supplementary software in treatment planning systems.

Acknowledgment

This research was performed using research grant of Shiraz University.

References

- Ghiassi-Nejad M, Jafarizadeh M, Ahmadian-Pour MR, Ghahramani AR. Dosimetric characteristics of ¹⁹²Ir sources used in interstitial brachytherapy. *Applied Radiation and Isotopes*. 2001 Aug 1;55(2):189-95. [https://doi.org/10.1016/S0969-8043\(00\)00375-4](https://doi.org/10.1016/S0969-8043(00)00375-4).
- Khan FM, Gibbons JP. *Khan's the physics of radiation therapy*. Lippincott Williams & Wilkins. 2014.
- Podgorsak EB. *Radiation oncology physics: a handbook for teachers and students*. *British journal of cancer*. 2008;98(5):71-99. <https://doi.org/10.1038/sj.bjc.6604224>.
- Orton CG. Time-dose factors (TDFs) in brachytherapy. *The British journal of radiology*. 1974 Sep;47(561):603-7. <https://doi.org/10.1259/0007-1285-47-561-603>.
- Rivard MJ, Coursey BM, DeWerd LA, Hanson WF, Saiful Huq M, Ibbott GS, and et al.. Update of AAPM Task Group No. 43 Report: A revised AAPM protocol for brachytherapy dose calculations. *Medical physics*. 2004 Mar;31(3):633-74. <https://doi.org/10.1118/1.1646040>.
- Sina S, Faghihi R, Meigooni AS, Mehdizadeh S, Zehtabian M, Mosleh-Shirazi MA. Simulation of the shielding effects of an applicator on the AAPM TG-43 parameters of ¹³⁷Cs Selectron LDR brachytherapy sources. *International Journal of Radiation Research*. 2009 Dec 1;7(3):135.
- Sina S, Faghihi R, Soleymani Meigooni A. A Comparison of the Dosimetric Parameters of ¹³⁷Cs Brachytherapy Source in Different Tissues with Water Using Monte Carlo Simulation. *Iranian Journal of Medical Physics*. 2012;9(1):65-74. <https://dx.doi.org/10.22038/ijmp.2012.331>.
- Meigooni AS, Meli JA, Nath R. Interseed effects on dose for ¹²⁵I brachytherapy implants. *Medical physics*. 1992 Mar;19(2):385-90. <https://doi.org/10.1118/1.596871>.
- Mason J, Al-Qaisieh B, Bownes P, Henry A, Thwaites D. Investigation of interseed attenuation and tissue composition effects in ¹²⁵I seed implant prostate brachytherapy. *Brachytherapy*. 2014 Nov 1;13(6):603-10. <https://doi.org/10.1016/j.brachy.2014.04.004>.
- Safigholi H, Shah A, Meigooni AS. A Novel Algorithm Accounting for Inter-Seed Attenuation Effect in Brachytherapy Treatment Planning Systems by Monte Carlo and Artificial Neural Networks. *Brachytherapy*. 2014 Mar 1;13:S27-8. <https://doi.org/10.1016/j.brachy.2014.02.237>.
- Sina S, Faghihi R, Meigooni A. Extracting Material Information from the CT Numbers by Artificial Neural Networks for Use in the Monte Carlo Simulations of Different Tissue Types in Brachytherapy. *Journal of Biomedical Physics and Engineering*. 2013; 3(1): 3-8.
- NV Dehkordi A., Sina S. Khodadadi F. A Comparison of Deep Learning and Pharmacokinetic Model Selection Methods in Segmentation of High-Grade Glioma. *Frontiers in biomedical technologies*. 2021; 8(1): 50-60. <https://www.sid.ir/en/journal/ViewPaper.aspx?id=841659>.
- Shen C, Gonzalez Y, Klages P, Qin N, Jung H, Chen L, et al. Intelligent inverse treatment planning via deep reinforcement learning, a proof-of-principle study in high dose-rate brachytherapy for cervical cancer. *Phys. Med. Biol*. 2019; 64(11): 115013. <https://doi.org/10.1088/1361-6560/ab18bf>
- Mao X, Pineau J, Keyes R, and. Enger S. A. RapidBrachyDL: rapid radiation dose calculations in brachytherapy via deep learning. *Int. J. Radiat. Oncol. Biol. Phys*. 2020; 108(3): 802–12. <https://doi.org/10.1016/j.ijrobp.2020.04.045>.
- Yusufaly TI, Kallis K, Simon A, Mayadev J, Yashar CM, Einck JP, et al. A knowledge-based organ dose prediction tool for brachytherapy treatment planning of patients with cervical cancer. *Brachytherapy*. 2020; 19(5): 624–34. <https://doi.org/10.1016/j.brachy.2020.04.008>
- Menhaj M. B. *Fundamentals of neural networks*. Tehran: Amirkabir university; 12th edition, spring 2018.